

Disintegration of Magnetic Flux in Decaying Sunspots as Observed with the *Hinode* SOT

M. Kubo¹, B. W. Lites¹, K. Ichimoto², T. Shimizu³, Y. Suematsu², Y. Katsukawa², T. D. Tarbell⁴, R. A. Shine⁴, A. M. Title⁴, S. Nagata⁵

and

S. Tsuneta²

kubo@ucar.edu

ABSTRACT

Continuous observations of sunspot penumbrae with the Solar Optical Telescope aboard *Hinode* clearly show that the outer boundary of the penumbra fluctuates around its averaged position. The penumbral outer boundary moves inward when granules appear in the outer penumbra. We discover that such granules appear one after another while moving magnetic features (MMFs) are separating from the penumbral “spines” (penumbral features that have stronger and more vertical fields than those of their surroundings). These granules that appear in the outer penumbra often merge with bright features inside the penumbra that move with the spines as they elongate toward the moat region. This suggests that convective motions around the penumbral outer boundary are related to the disintegration of magnetic flux in the sunspot. We also find that dark penumbral filaments frequently elongate into the moat region in the vicinity of MMFs that detach from penumbral spines. Such elongating dark penumbral filaments correspond to nearly horizontal fields extending from the penumbra. Pairs of MMFs with positive and negative polarities are sometimes observed along the elongating

¹High Altitude Observatory, National Center for Atmospheric Research, P.O. Box 3000, Boulder, CO 80307. The National Center for Atmospheric Research is sponsored by the National Science Foundation.

²National Astronomical Observatory of Japan, 2-21-1 Osawa, Mitaka, Tokyo 181-8588, Japan.

³Institute of Space and Astronautical Science, JAXA, Sagami-hara, Kanagawa 229-8510, Japan.

⁴Lockheed Martin Solar and Astrophysics Laboratory, Building 252, 3251 Hanover Street, Palo Alto, CA 94304.

⁵Hida Observatory, Kyoto University, Takayama, Gifu 506-1314, Japan.

dark penumbral filaments. This strongly supports the notion that such elongating dark penumbral filaments have magnetic fields with a “sea serpent”-like structure. Evershed flows, which are associated with the penumbral horizontal fields, may be related to the detachment of the MMFs from the penumbral spines, as well as to the formation of the MMFs along the dark penumbral filaments that elongate into the moat region.

Subject headings: Sun: granulation — Sun: magnetic fields — Sun: photosphere — (Sun:) sunspots

1. INTRODUCTION

Sunspot penumbrae consist of many dark and bright radial filaments. The inclination of penumbral magnetic fields fluctuates with azimuthal angle around the spot center (Degenhardt & Wiehr 1991; Title et al. 1993; Lites et al. 1993; Stanchfield et al. 1997; Westendorp Plaza et al. 2001a,b; Bello González et al. 2005; Langhans et al. 2005). The bright penumbral filaments have magnetic fields that are more vertical than those of the dark penumbral filaments in the outer penumbra. The vertical and horizontal components of the penumbral fields have been called a “penumbral spine” and a “penumbral intra-spine,” respectively (Lites et al. 1993). Radial flows and radial motions are also observed in the penumbra. The Evershed flow is a horizontal outward flow along the horizontal component of the penumbral magnetic fields (Degenhardt & Wiehr 1991; Title et al. 1993; Lites et al. 1993; Rimmele 1995; Stanchfield et al. 1997; Westendorp Plaza et al. 2001a,b; Bellot Rubio et al. 2003, 2004; Borrero et al. 2004, 2005; Cabrera Solana et al. 2006, 2007, 2008). Evershed flows with supersonic velocities are sometimes inferred around the outer boundary of the penumbra (del Toro Iniesta et al. 2001), and are observed directly (Shimizu et al. 2008b). Penumbral grains, which are patchy bright features, move toward the umbra in the inner penumbra, and the penumbral grains in the outer penumbra show both inward and outward motions (e.g. Sobotka et al. 1999; Sobotka & Sütterlin 2001; Bovelet & Wiehr 2003). The Evershed flow appears to originate at the inward-moving penumbral grains in the inner penumbra (Rimmele & Marino 2006; Ichimoto et al. 2007). Various models have been proposed to explain the complex magnetic and velocity fields of penumbrae (e.g., Solanki & Montavon 1993; Schlichenmaier et al. 1998; Thomas et al. 2002; Spruit & Scharmer 2006; Heinemann et al. 2007).

Radial outward flows are dominant in the moat region that surrounds mature sunspots. Moving magnetic features (MMFs) are small magnetic elements that have sizes of typically less than $2''$ in the moat region (Sheeley 1969; Vrabc 1971; Harvey & Harvey 1973).

MMFs mostly appear around the penumbral outer boundary and then move almost radially outward in the moat region for mature and decaying sunspots (Harvey & Harvey 1973; Ryutova et al. 1998; Zhang et al. 2003; Sainz Dalda & Martínez Pillet 2005; Ravindra 2006). The lifetimes of MMFs range from a few minutes to 10 hr (Vrabec 1974; Zhang et al. 2003; Hagenaar & Shine 2005). Those MMFs with longer lifetimes may reach the outer boundary of the moat region. Recent observations suggest that MMFs located on lines extrapolated outward from the horizontal component of the penumbral magnetic fields into the moat region correspond to the photospheric intersections of undulating horizontal fields extending from the penumbra (Sainz Dalda & Martínez Pillet 2005; Cabrera Solana et al. 2006, 2007; Kubo et al. 2007a). This supports the “sea serpent” concept for MMFs, whereby the horizontal penumbral fields undulate into and out of the solar surface (Harvey & Harvey 1973; Schlichenmaier 2002). Many authors have proposed that the fluctuating penumbral fields and the subsequent MMFs are produced by Evershed flows (e.g., Ryutova et al. 1998; Martínez Pillet 2002; Thomas et al. 2002; Schlichenmaier 2002; Zhang et al. 2003, 2007b; Cabrera Solana et al. 2006). On the other hand, MMFs located on the lines extrapolated from the penumbral spines have magnetic fields that are more vertical than those of their surroundings (Kubo et al. 2007a). Such MMFs appear to be formed as a result of the detachment of a fraction of the magnetic field from the penumbral spines.

The net magnetic flux transported by all the MMFs exceeds the flux-loss rate of the sunspot (Martínez Pillet 2002; Kubo et al. 2007a). Hence, it has been suggested that the MMFs detached from the penumbral spines alone are the agent that removes magnetic flux from the sunspot (e.g., Shine & Title 2001; Martínez Pillet 2002; Thomas et al. 2002; Weiss et al. 2004). Those MMFs might carry away an amount of magnetic flux sufficient to account for the flux loss of the sunspot (Kubo et al. 2007a). If so, the formation of those MMFs that detach from the penumbral spines is more important to the process of sunspot decay than that of other types of MMFs.

Kubo et al. (2007b) found that bright features (granules) appear where an MMF is separating from the penumbral spine, but only one event was examined in detail in that work. Using observations of two mature sunspots made by the Solar Optical Telescope (SOT; Tsuneta et al. 2008; Suematsu et al. 2008; T. D. Tarbell et al. 2008 in preparation; Ichimoto et al. 2008; Shimizu et al. 2008a) aboard the *Hinode* satellite (Kosugi et al. 2007), we build statistics of the comparison between MMFs detaching from the spines and both bright and dark features around the penumbral outer boundary. The *Hinode* SOT reveals the evolution of fine structures in both the penumbra and the moat region from continuous observations with a spatial resolution of $0.2'' - 0.3''$.

2. OBSERVATIONS

We focus on SOT observations of two mature sunspots that were located near the disk center in order to be able to clearly identify the penumbral spines and intra-spines with line-of-sight magnetograms. These sunspots are typical decaying sunspots that have a nearly circular shape. The data sets used in this study are summarized in Table 1. We use the observations of the sunspot in NOAA Active Region (AR) 10933 to investigate temporal evolution in the G-band intensity and line-of-sight magnetic fields in the photosphere over a large field of view. The temporal evolution of the vector magnetic field is obtained by the *Hinode* Spectropolarimeter (SP) for the sunspot in NOAA AR 10944. These data complement the G-band sequences with quantitative measures of the vector field, but over a small field of view.

2.1. Active Region NOAA 10933

The filtergram (FG) of the SOT obtained sunspot images continuously in NOAA AR 10933 with a 2 minute cadence from 16:14 to 24:00 on 2007 January 4, and with a 7 minute cadence from 0:00 to 4:00 on 2007 January 5. The broadband filter imager (BFI) provided G-band 4305 Å and Ca II H 3968 Å images over the full field of view ($223'' \times 112''$). The narrowband filter imager (NFI) observed the intensity (Stokes I) and circular polarization (Stokes V) at -120 mÅ from the center of the photospheric line Fe I 6302.5 Å with the full field of view ($328'' \times 164''$). The filtergram images were binned 2×2 pixels from the full resolution in this observation. The size of a binned pixel was $0.108''$ for the BFI and $0.16''$ for the NFI, respectively.

The SP obtained a spatial distribution of the full polarization state (Stokes I , Q , U , and V) with the Fast Map mode from 18:40 to 19:43. Having SP observations of the full polarization state permitted us to infer the magnetic field vector and thermodynamic parameters in the photosphere. In the Fast Map mode, the slit-scanning step was $0.297''$, and a pixel sampling along the slit was $0.320''$. The field of view was $297'' \times 164''$. The Stokes profiles of two magnetically sensitive Fe lines at 6301.5 and 6302.5 Å were obtained simultaneously with a wavelength sampling of 21.6 mÅ and an integration time of 3.2 seconds for each slit position. Repeated observations for an area of $3.9'' \times 82''$ were also carried out from 21:57 to 22:50. The evolution of the magnetic fields in this small area was reported in Kubo et al. (2007b).

2.2. Active Region NOAA 10944

The sunspot in NOAA AR 10944 was observed simultaneously with the FG and the SP for 6 hr from 11:51 on 2007 February 27. The BFI provided full-resolution images for the G-band and the Ca II H line with a field of view of $56'' \times 56''$. The NFI observed the Stokes I and V of the photospheric line Fe I 6302.5 Å in the shutterless mode, in which continuous readout was performed for the central area of the CCD and the outer parts of the CCD were masked. The polarization accuracy was better in the shutterless mode, but the field of view was narrow ($32'' \times 81''$). The time cadence of the BFI and NFI was 1 minute.

The SP repeatedly scanned the same region of $9.5'' \times 82''$ with the Normal Map mode. In the Normal Map mode, the spatial sampling was $0.149'' \times 0.160''$, and the integration time for each slit position was 4.8 seconds. The SP took about 5.5 minutes to obtain each map.

3. DATA ANALYSIS

3.1. Filtergrams

The standard calibrations, which were dark subtraction, flat-fielding, and bad pixel correction, were performed for the G-band images with the BFI. Only dark subtraction was applied for the Stokes I images with the NFI, because flat-fielding data for the NFI images were not yet available for these data sets. Hereafter, we denote the Stokes V image divided by the Stokes I image obtained at the same time as a “line-of-sight magnetogram.” The effect of flat-fielding on the line-of-sight magnetogram is small. Image cross-correlation allowed us to align the calibrated G-band images to a reference image in order to remove the drift due to the correlation tracker (Shimizu et al. 2008a) and the sunspot proper motion. The image taken at the time of the midpoint of all the G-band images was used as the reference. The line-of-sight magnetograms (Stokes V/I) were aligned to the G-band images that were taken at the time closest to the time of the NFI observations via cross-correlation of the G-band to the Stokes I images.

On the G-band image for NOAA AR 10933, Figure 1 shows the locations that we determined for the time-averaged penumbral outer boundary, the geometrical center of the sunspot, and the reference frame for the position angles around the sunspot center. The image averaged over all the G-band images was used to evaluate the average intensities of the quiet area, the penumbral outer boundary, and the central area of the sunspot. The quiet-area intensity (I_0) was determined by a Gaussian fit to the distribution of the intensities for pixels located well outside the sunspot. We spatially smoothed the averaged G-band image

with a box of $5'' \times 5''$ to remove local fluctuations due to penumbral fine structure. Let I_G be the smoothed G-band intensity. We then define the average penumbral outer boundary as the locus of $I_G = 0.87I_0$. In NOAA AR 10933, the sunspot center was chosen as the center of gravity (COG) of the $I_0 - I_G$ image for the entire sunspot. For NOAA AR 10944, we use the COG of the $I_0 - I_G$ image for the umbra ($I_G < 0.4$) only because the images did not cover the entire penumbral area.

We used only the southern part for the sunspot in NOAA AR 10933, because a largest bubble was stably located at the top of the NFI images (T. D. Tarbell et al. 2008, in preparation). The southern part of the sunspot appeared to be clean.

3.2. Spectropolarimeter

We performed the following calibrations for the Stokes profiles observed with the SP: (1) dark subtraction and flat-fielding, (2) the polarization calibration induced by the optical elements in the SOT, (3) the correction in the direction of spectral dispersion, (4) merging of two orthogonal polarizations simultaneously measured with the left and right segments of the CCD, (5) the correction for spectral curvature, (6) compensation for residual crosstalk $I \rightarrow QUV$, (7) the correction for the orbital shift in the wavelength and slit directions due to the thermal flexure of the Focal Plane Package (FPP; T. D. Tarbell et al. 2008, in preparation), and (8) an intensity correction due to the slit width variation along the slit. After the calibration, vector magnetic fields were derived with a least-squares fitting (“Stokes inversion”) that assumed a Milne-Eddington representation of the atmospheric stratification (T. Yokoyama et al. 2008, in preparation). Of the 13 parameters obtained with the Stokes inversion, we consider only the field strength ($|\mathbf{B}|$), the inclination angle relative to the line of sight (γ), and the filling factor (f). The magnetic field maps thus obtained were aligned to the G-band images taken at the time closest to the midpoint of the SP maps, using cross-correlation of the SP continuum intensity map with the BFI G-band images.

One must resolve the 180° ambiguity of the azimuth angle in order to calculate the inclination with respect to the normal to the solar surface. We first select the line-of-sight azimuth closest to the potential field computed using the line-of-sight component of the magnetic field as a boundary condition. Then we interactively determined the azimuth to reduce discontinuities of azimuth and inclination angles by using the AZAM utility (written in IDL by P. Seagraves; Lites et al. 1995), which allowed us to display and select the two alternatives for the azimuth angle. Both the sunspots were located near the disk center, so any errors in the inclination arising from the wrong choice of the ambiguous azimuth will amount to less than 15° . In any event, an erroneous choice of azimuth is rare for symmetric

sunspots such as those studied here.

4. RESULTS

4.1. Magnetic Fields of Bright/Dark Features in the Outer Penumbra

The penumbra consists of many radial structures, and MMFs usually move radially outward from the outer penumbral edge. Figure 2 displays on the vertical axis the radial distance from the averaged penumbral outer boundary, and on the horizontal axis, the position angle around the sunspot center. The contours in Figure 2 enclose features brighter in the G band than $0.87I_0$. Many of the features enclosed by the contours in Figure 2a may be found in the middle and outer penumbra. Some of these correspond to stronger positive line-of-sight fields (Fig. 2b). Furthermore, Figure 2c demonstrates that the enclosed radial structures have magnetic fields that are more vertical than those of their surroundings. The line-of-sight direction is nearly normal to the solar surface in this case. Therefore, we can assign the white and gray areas in the outer penumbra of Figure 2b as the vertical (spine) component and the horizontal (intra-spine) component of the penumbral magnetic fields, respectively. We can also identify the patchy magnetic elements in Figure 2b that have intense white and black areas in the moat region as MMFs with vertical fields.

Bright features in the G-band images usually have a radially elongated structure. Langhans et al. (2005) showed, using the finest spatial resolution ($0.2''$) ever achieved, that bright penumbral filaments have more vertical magnetic fields than those of dark penumbral filaments in the outer penumbra. We confirm this relationship using spectropolarimetric measurements with a spatial resolution of $0.3''$.

4.2. MMFs Separating from the Penumbra

We find a clear correspondence between MMFs separating from the penumbral spines and convective motions in the outer penumbra. Figure 3 shows a time series of G-band images and line-of-sight magnetograms around the position angle of 212° (indicated by the vertical lines in Fig. 2). A penumbral spine appears in the frame at 18:46, as shown by the arrow pointing to the left, and it elongates radially outward. In the same period, a bright elongated structure appears in the G-band image, and its brightest area also moves outward with the elongating penumbral spine. The elongating spine connects with an existing magnetic element (indicated by the arrow pointing to the right) from 19:46 to 20:46, and the outer part of the elongating spine becomes large in this period. The outer part of the

elongating spine is gradually separating from the main body of the spine, and then this part becomes an MMF in the frame at 23:46. We find that granules appear in the outer penumbra when the outer edge of the elongating spine reaches the penumbra outer boundary (see the 21:46 frame). Such granules continuously appear one after another while the MMF is detaching from the spine.

Figure 4 shows the temporal change of the G-band intensity and the line-of-sight magnetic field along a radial line at the position angle of 212° . Two kinds of magnetic elements with outward motion can be seen from the outer penumbra to the inner moat region, as reported in Zhang et al. (2007a): fuzzy, small magnetic elements move quickly, and large magnetic elements move slowly. There is no significant G-band bright feature in the outer and middle penumbra, and only the fuzzy magnetic elements are visible there in the first 2 hr. Then, a bright feature appears around 18:00 on January 4 and moves toward the moat region with an elongating large magnetic element, which corresponds to the elongating penumbral spine shown in Figure 3. The bright feature divides into two features around 19:00: one moves toward the umbra (the upward arrow in Fig. 4a), and the other moves outward with the elongating spine to become an MMF (downward arrow). The bright feature moving outward disappears around 20:00, and another bright feature subsequently appears 20 minutes later at a position similar to where the previous feature disappeared. This new bright feature also moves outward with the elongating spine. The outer edge of the spine arrives at the penumbral outer boundary around 22:00, and as a result of the appearance of granules in the outer penumbra, the penumbral outer boundary retracts toward the umbra relative to its average position. The bright feature moving with the elongating spine merges with the appearing granules. The outer part of the elongating spine is completely separated from the penumbra around 00:00, and this part still moves outward as an MMF. The elongating speed of the spine averaged over 6 hr after its appearance is about 0.2 km s^{-1} , which is similar to the horizontal velocities of MMFs that have vertical magnetic fields with the same polarity as that of the sunspot around the penumbral outer boundary (Kubo et al. 2007a). There are many bright features moving inward and outward in the penumbra before 00:00 on January 5, but most of the bright features and the elongating spine disappear from the outer penumbra after the MMF separates from the penumbral spine.

The relationship between the MMF separating from the elongated spine and convection in the outer penumbra is demonstrated above for only the radial line at the position angle of 212° . To confirm that this relationship is common all around the penumbral outer boundary, we compare the temporal change in the G-band intensity to the line-of-sight magnetic field at $2''$ inside the penumbral outer boundary for position angles ranging from 180° to 360° in Figure 5. There are many bright streaks in Figure 5a. These bright streaks represent the granules appearing in the outer penumbra or the penumbral bright features moving outward.

On the other hand, the positive magnetic features in Figure 5*b* mostly correspond to the elongating spines or the MMFs detaching from the spines. We confirm that the G-band bright streaks are generally located at the elongating spines or at the detaching MMFs, as shown by the contours in Figure 5. This tendency is more clearly seen in the limb-side penumbra (the left-hand side of Fig. 5) than in the center-side penumbra due to the projection effect.

Some bright features are not located at positive magnetic features but at negative magnetic features with weak magnetic fields (darker features than their surroundings; see the green boxes in Fig. 5). The bright features in the outer penumbra are related to formation of the MMFs that have the polarity opposite to that of the sunspot.

4.3. Dark Penumbra Filament Elongating to the Moat Region

The outer boundary of the penumbra fluctuates around its average position, and dark penumbral filaments often elongate into the moat region. Such dark filaments correspond to the areas with strong horizontal fields that extend from the penumbra. The arrows in Figure 6 indicate the evolution of three dark, elongating penumbral filaments with strong horizontal fields in NOAA AR 10944. The longer dark penumbral filaments extend to the outer moat region. The MMFs with the polarity opposite to that of the sunspot are located at the outer edge of the filamentary structure with strong horizontal fields. This is consistent with the result of Kubo et al. (2007b). The dotted circles in the rightmost frames of Figures 6*b* and 6*c* indicate that two MMFs with positive polarity and two MMFs with negative polarity are aligned along each of two filamentary structures that have a strong horizontal field (the middle circles each contain two MMFs that have opposite polarities). This is clear evidence that bipolar MMFs correspond to the intersections of the solar surface with serpentine horizontal fields extending from the penumbra. In this case, each serpentine horizontal field line consists of both Ω -loops and U-loops (see Fig. 8*b*). This means that whether bipolar MMFs form Ω -loops or U-loops depends on which segments of the extended penumbral fields are chosen, as well as on the number of intersections. The bipolar MMFs with a U-loop may correspond to a localized dip of the magnetic canopy, as proposed by Zhang et al. (2003).

Figure 7 shows the temporal change in the G-band intensity and the line-of-sight magnetic field at $1''$ outside the penumbral outer boundary of NOAA AR 10933. The dark penumbral filaments elongating to the moat region are indicated by the dark features in Figure 7*a*. The appearance and disappearance of the long positive magnetic features in Figure 7*b* are mainly due to the outward motion of MMFs that detach from the penumbral spines. The elongating dark filaments (red contours in Fig. 7*b*) are usually located at the

areas that have nearly horizontal magnetic fields with respect to the solar surface (gray or weak white areas in Fig. 7*b*). We find that most of the elongating dark filaments are adjacent to the MMFs that have the same polarity as the sunspot. This means that the dark penumbral filaments elongate near the MMFs that have the same polarity as the sunspot when such MMFs separate from the penumbra. One example of such a dark penumbral filament and an MMF can be seen at 22:46 in Figure 3.

5. SUMMARY AND DISCUSSION

The SOT allows us to perform continuous observations with high spatial resolution for a duration longer than the typical lifetime of MMFs. The results regarding flux removal from the sunspot in this study are summarized as follows (see also Fig. 8):

1. G-band bright features in the outer penumbra are located at the elongating spines or at the MMFs detaching from the spines. G-band bright features moving both outward and inward can be found in the middle and outer penumbra. The penumbral spines elongate toward the moat region in concert with the outward motions of the penumbral bright features.
2. Granules appear in the outer penumbra at locations where MMFs that have the same polarity as the sunspot separate from the penumbral spines. Such granules often merge with bright features moving along the elongating spines.
3. Dark penumbral filaments frequently elongate into the moat region, and longer ones reach the outer moat region. The elongating dark penumbral filaments coincide with filamentary structures that have strong horizontal fields that extend outward from the penumbra. We present clear examples of bipolar MMFs indicating a serpentine field with multiple intersections with the solar photosphere. MMFs with positive and negative polarities are located along the filamentary structures with strong horizontal fields.
4. The MMFs that are detached from the penumbral spines are usually observed in the neighborhood of the elongating dark penumbral filaments.

The total flux transport rate by the MMFs that are detached from the penumbral spines is greater than the flux-loss rate of the sunspot (Kubo et al. 2007a). Therefore, items 1 and 2 above confirm that convection in the outer penumbra is related to the flux removal of the sunspot (Kubo et al. 2007b). However, the magnetic energy density of the penumbral fields is

larger than the kinetic energy density of the penumbral bright features at the photospheric surface. Converging and downward flows are inferred in the subsurface convection zone around a stable sunspot (Zhao et al. 2001), and such flows might be essential to the formation and sustenance of sunspots (Meyer et al. 1974; Parker 1979, 1992). The appearance of the bright features moving outward in the outer penumbra suggests subsurface upwelling and diverging flows. Such flows would work against the stabilization of the sunspot, and recent MHD simulations showed that magnetic flux is carried away from the spot by subsurface diverging flows (Heinemann et al. 2007). Meyer et al. (1974) suggested that small flux tubes diffuse out into the moat region by small scale convection beneath the sunspot. The fact that the bright features and granules appear in the outer penumbra at the location of the elongating spines (that subsequently become MMFs) supports this idea.

Another possibility is that Evershed flows detach penumbral flux and advect it into the moat region. Evershed flows with supersonic velocities are often observed around the penumbral outer boundary (Shimizu et al. 2008b). Supersonic flows are also observed in connection with horizontal fields extending from the penumbra (Kubo et al. 2007b). The kinetic energy density of such supersonic flows is larger than the magnetic energy density of the magnetic fields in the outer penumbra. Nevertheless, the *Hinode* SP observations of vector magnetic fields with 0.3'' resolution have confirmed that the Evershed flows are radial outward flows along those penumbral filaments that have nearly horizontal fields (Ichimoto et al. 2007). Detachment of the MMFs is observed when the penumbral horizontal fields elongate into the moat region. This means that Evershed flows are related not only to the formation of the bipolar MMFs located along the extending penumbral horizontal fields, but also to the detachment of the MMFs from the penumbral spines. The Evershed flows originate at penumbral bright features that are moving inward in the inner penumbra (Rimmele & Marino 2006; Ichimoto et al. 2007), and the detachment of MMFs from the penumbra is observed with penumbral bright features that are moving outward in the outer penumbra. This suggests the possibility that both Evershed flows and the detachment of MMFs originate from the activity of convection below the sunspot penumbra. The relationship between Evershed flows and sunspot decay also should be investigated using Doppler and magnetic field measurements of both high spatial and high temporal resolution.

The authors would like to acknowledge the late Professor T. Kosugi and all the members of the *Hinode* team for their work to realize a successful mission. We also thank T. Yokoyama and M. Shimojo for their help in deriving the magnetic field vector. R. Centeno is also thanked for the co-alignment method between the G-band images and the SP maps. *Hinode* is a Japanese mission developed and launched by ISAS/JAXA, with NAOJ as domestic partner and NASA and STFC (UK) as international partners. It is operated by these

agencies in cooperation with ESA and NSC (Norway). This work was partly carried out at the NAOJ *Hinode* Science Center, which is supported by the Grant-in-Aid for Creative Scientific Research “The Basic Study of Space Weather Prediction” from MEXT, Japan (Head Investigator: K. Shibata), generous donations from Sun Microsystems, and NAOJ internal funding.

REFERENCES

- Bello González, N., Okunev, O. V., Domínguez Cerdeña, I., Kneer, F., & Puschmann, K. G. 2005, *A&A*, 434, 317
- Bellot Rubio, L. R., Balthasar, H., Collados, M., & Schlichenmaier, R. 2003, *A&A*, 403, L47
- Bellot Rubio, L. R., Balthasar, H., & Collados, M. 2004, *A&A*, 427, 319
- Borrero, J. M., Solanki, S. K., Bellot Rubio, L. R., Lagg, A., & Mathew, S. K. 2004, *A&A*, 422, 1093
- Borrero, J. M., Lagg, A., Solanki, S. K., & Collados, M. 2005, *A&A*, 436, 333
- Bovelet, B., & Wiehr, E. 2003, *A&A*, 412, 249
- Cabrera Solana, D., Bellot Rubio, L. R., Beck, C., & del Toro Iniesta, J. C. 2006, *ApJ*, 649, L41
- Cabrera Solana, D., Bellot Rubio, L. R., Beck, C., & Del Toro Iniesta, J. C. 2007, *A&A*, 475, 1067
- Cabrera Solana, D., Bellot Rubio, L. R., Borrero, J. M., & Del Toro Iniesta, J. C. 2008, *A&A*, 477, 273
- del Toro Iniesta, J. C., Bellot Rubio, L. R., & Collados, M. 2001, *ApJ*, 549, L139
- Degenhardt, D. & Wiehr, E. 1991, *A&A*, 252, 821
- Hagenaar, H. J., & Shine, R. A. 2005, *ApJ*, 635, 659
- Harvey, K. & Harvey, J. 1973, *Sol. Phys.*, 28, 61
- Heinemann, T., Nordlund, Å., Scharmer, G. B., & Spruit, H. C. 2007, *ApJ*, 669, 1390
- Ichimoto, K., et al. 2007, *PASJ*, 59, S593

- Ichimoto, K., et al. 2008, *Sol. Phys.*, in press.
- Kosugi, T., et al. 2007, *Sol. Phys.*, 243, 3
- Kubo, M., Shimizu, T., & Tsuneta, S. 2007a, *ApJ*, 659, 812
- Kubo, M., et al. 2007b, *PASJ*, 59, S607
- Langhans, K., Scharmer, G. B., Kiselman, D., Löfdahl, M. G., & Berger, T. E. 2005, *A&A*, 436, 1087
- Lites, B. W., Elmore, D. F., Seagraves, P., & Skumanich, A. P. 1993, *ApJ*, 418, 928
- Lites, B. W., Low, B. C., Martínez Pillet, V., Seagraves, P., Skumanich, A., Frank, Z. A., Shine, R. A., & Tsuneta, S. 1995, *ApJ*, 446, 877
- Martínez Pillet, V. 2002, *Astronomische Nachrichten*, 323, 342
- Metcalf, T. R., et al. 2006, *Sol. Phys.*, 237, 267
- Meyer, F., Schmidt, H. U., Wilson, P. R., & Weiss, N. O. 1974, *MNRAS*, 169, 35
- Parker, E. N. 1979, *ApJ*, 230, 905
- Parker, E. N. 1992, *ApJ*, 390, 290
- Ravindra, B. 2006, *Sol. Phys.*, 237, 297
- Rimmele, T. R. 1995, *ApJ*, 445, 511
- Rimmele, T., & Marino, J. 2006, *ApJ*, 646, 593
- Ryutova, M., Shine, R., Title, A., & Sakai, J. I. 1998, *ApJ*, 492, 402
- Sainz Dalda, A., & Martínez Pillet, V. 2005, *ApJ*, 632, 1176
- Schlichenmaier, R., Jahn, K., & Schmidt, H. U. 1998, *A&A*, 337, 897
- Schlichenmaier, R. 2002, *Astronomische Nachrichten*, 323, 303
- Seagraves, P. 1995, HAO/NCAR internal report
- Sheeley, N. R., Jr. 1969, *Sol. Phys.*, 9, 347
- Shimizu, T., et al. 2008a, *Sol. Phys.*, in press.
- Shimizu, T et al. 2008b, *ApJ*, in press

- Shine, R., & Title, A. 2001, in *Encyclopedia of Astronomy and Astrophysics*, Vol. 4, ed. P. Murdin (Bristol: IoP), 3209
- Sobotka, M., Brandt, P. N., & Simon, G. W. 1999, *A&A*, 348, 621
- Sobotka, M., & Sütterlin, P. 2001, *A&A*, 380, 714
- Solanki, S. K., & Montavon, C. A. P. 1993, *A&A*, 275, 283
- Spruit, H. C., & Scharmer, G. B. 2006, *A&A*, 447, 343
- Stanchfield, D. C. H., Thomas, J. H., & Lites, B. W. 1997, *ApJ*, 477, 485
- Suematsu, Y., et al. 2008, *Sol. Phys.*, in press
- Thomas, J. H., Weiss, N. O., Tobias, S. M., & Brummell, N. H. 2002, *Nature*, 420, 390
- Title, A. M., Frank, Z. A., Shine, R. A., Tarbell, T. D., Topka, K. P., Scharmer, G., & Schmidt, W. 1993, *ApJ*, 403, 780
- Tsuneta, S., et al. 2008, *Sol. Phys.*, in press.
- Vrabc, D. 1971, in *IAU Symp. 43, Solar Magnetic Fields*, ed. R. Howard (Dordrecht: Reidel), 329
- Vrabc, D. 1974, in *IAU Symp. 56, Chromospheric Fine Structure*, ed. R. G. Athay (Dordrecht: Reidel), 201
- Weiss, N. O., Thomas, J. H., Brummell, N. H., & Tobias, S. M. 2004, *ApJ*, 600, 1073
- Westendorp Plaza, C., del Toro Iniesta, J. C., Ruiz Cobo, B., & Pillet, V. M. 2001a, *ApJ*, 547, 1148
- Westendorp Plaza, C., del Toro Iniesta, J. C., Ruiz Cobo, B., Pillet, V. M., Lites, B. W., & Skumanich, A. 2001b, *ApJ*, 547, 1130
- Zhang, J., Solanki, S. K., & Wang, J. 2003, *A&A*, 399, 755
- Zhang, J., Solanki, S. K., & Woch, J. 2007a, *A&A*, 475, 695
- Zhang, J., Solanki, S. K., Woch, J., & Wang, J. 2007b, *A&A*, 471, 1035
- Zhao, J., Kosovichev, A. G., & Duvall, T. L. 2001, *ApJ*, 557, 384

Table 1. Data Sets Used in This Study

NOAA AR	Location	Date	Period	SOT Observation	Field of view (arcsec)	Cadence (minutes)	Figure
10933	S02, E12	2007 Jan 04	16:14-24:00	BFI ^a (G-band)	223'' × 112''	2	1, 2, 3, 4, 5, 7
			16:14-24:00	NFI ^b (Stokes I, V)	328'' × 164''	2	2, 3, 4, 5, 7
			18:40-19:43	SP ^c	297'' × 164''	63 ^d	2
		2007 Jan 05	00:00-03:58	BFI (G-band)	223'' × 112''	7	4
10944	S01, E13	2007 Feb 27	00:00-03:58	NFI (Stokes I, V)	328'' × 164''	7	4
			11:57-17:54	BFI (G-band)	56'' × 56''	1	6
			11:51-17:51	SP	9.5'' × 82''	5.5 ^d	6

^aBroadband filter imager

^bNarrowband filter imager

^cSpectropolarimeter

^dCadence for one map

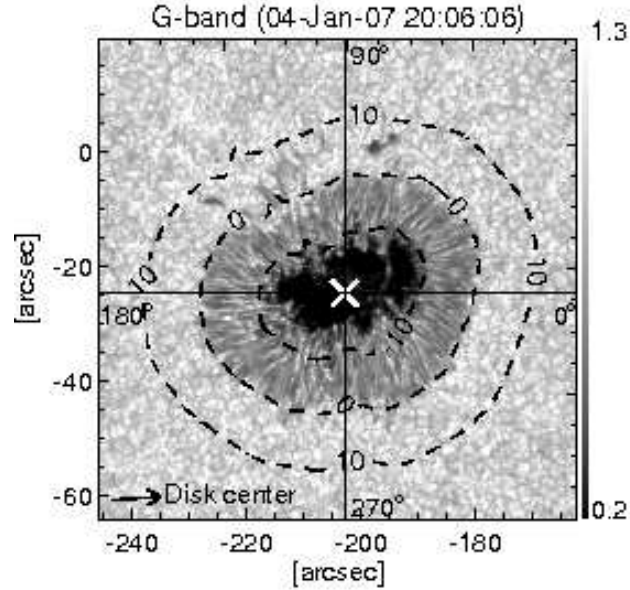


Fig. 1.— Sunspot in NOAA AR 10933, observed with the *Hinode* SOT. The gray-scale bar at the right indicates intensity normalized to the mean intensity of the quiet area outside the sunspot. The cross corresponds to the geometrical center of the sunspot. The solid lines show the position angle, measured counterclockwise from the solar west around the sunspot center. The three dashed lines correspond to distances of $-10''$, $0''$, and $10''$ from the penumbral outer boundary. The horizontal and vertical axes represent the positions with respect to the disk center.

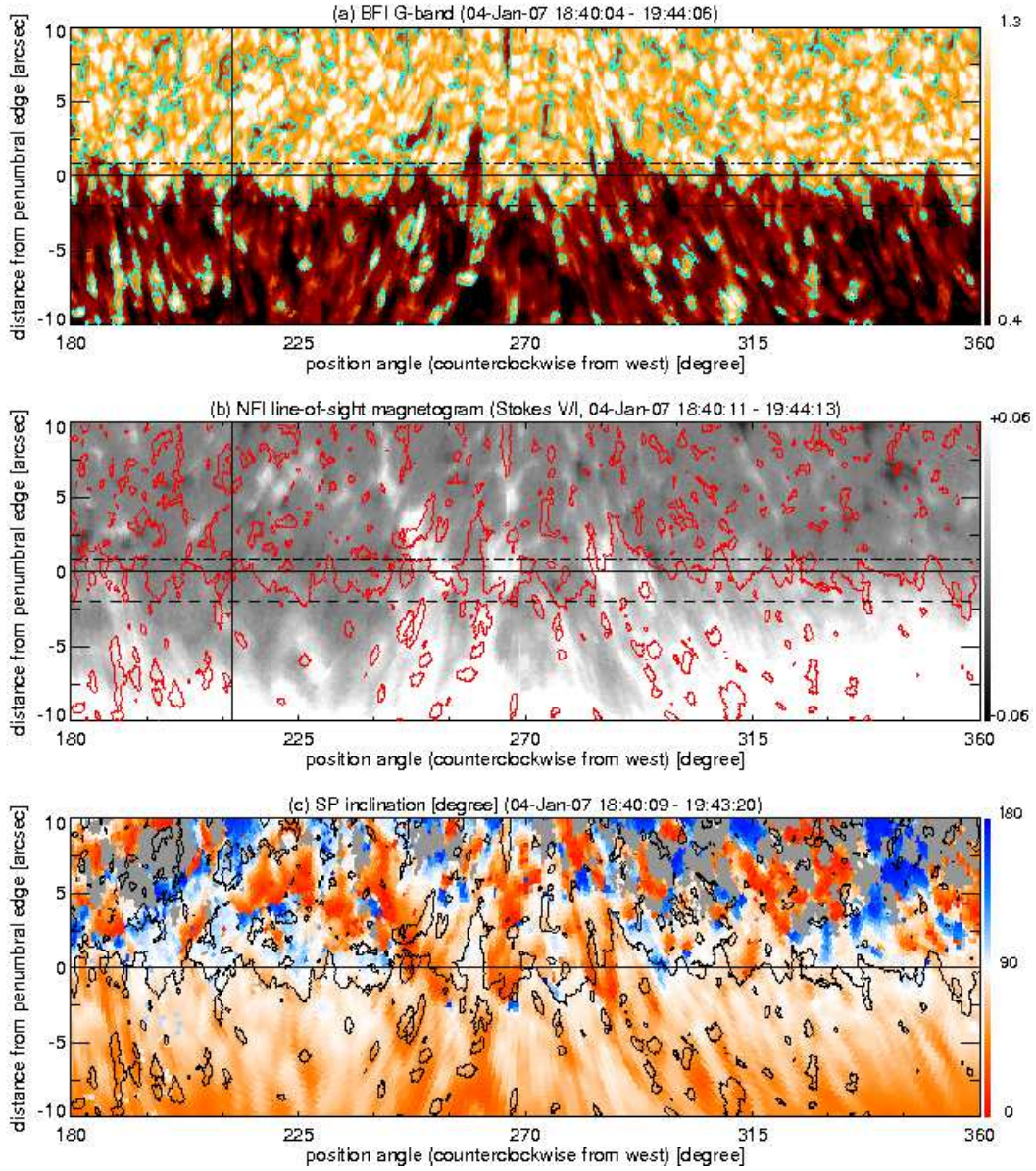


Fig. 2.— (a) G-band image, (b) line-of-sight magnetogram, and (c) magnetic field inclination. The vertical axis shows the radial distance from the penumbral outer boundary, and the horizontal axis shows the position angle around the sunspot center. These panels are made from the observations of NOAA AR 10933 on 2007 January 4. Each pixel in panels *a* and *b* was aligned to the time and position closest to those of each pixel in panel *c*. The G-band intensity is normalized to the quiet-area intensity. The contours represent a G-band intensity of 0.87. White (black) indicates positive (negative) polarity in panel *b*. An inclination of 90° corresponds to magnetic fields directed perpendicular to the local vertical, and inclinations of 0° and 180° represent magnetic fields directed away from the solar surface and magnetic fields directed toward the surface, respectively. The horizontal solid line shows the averaged outer boundary of the penumbra. The horizontal dashed and dash-dotted lines in panels *a* and *b* represent distances of $2''$ inside and $1''$ outside the outer penumbral boundary, respectively. The vertical solid line in panels *a* and *b* shows the position angle of 212° .

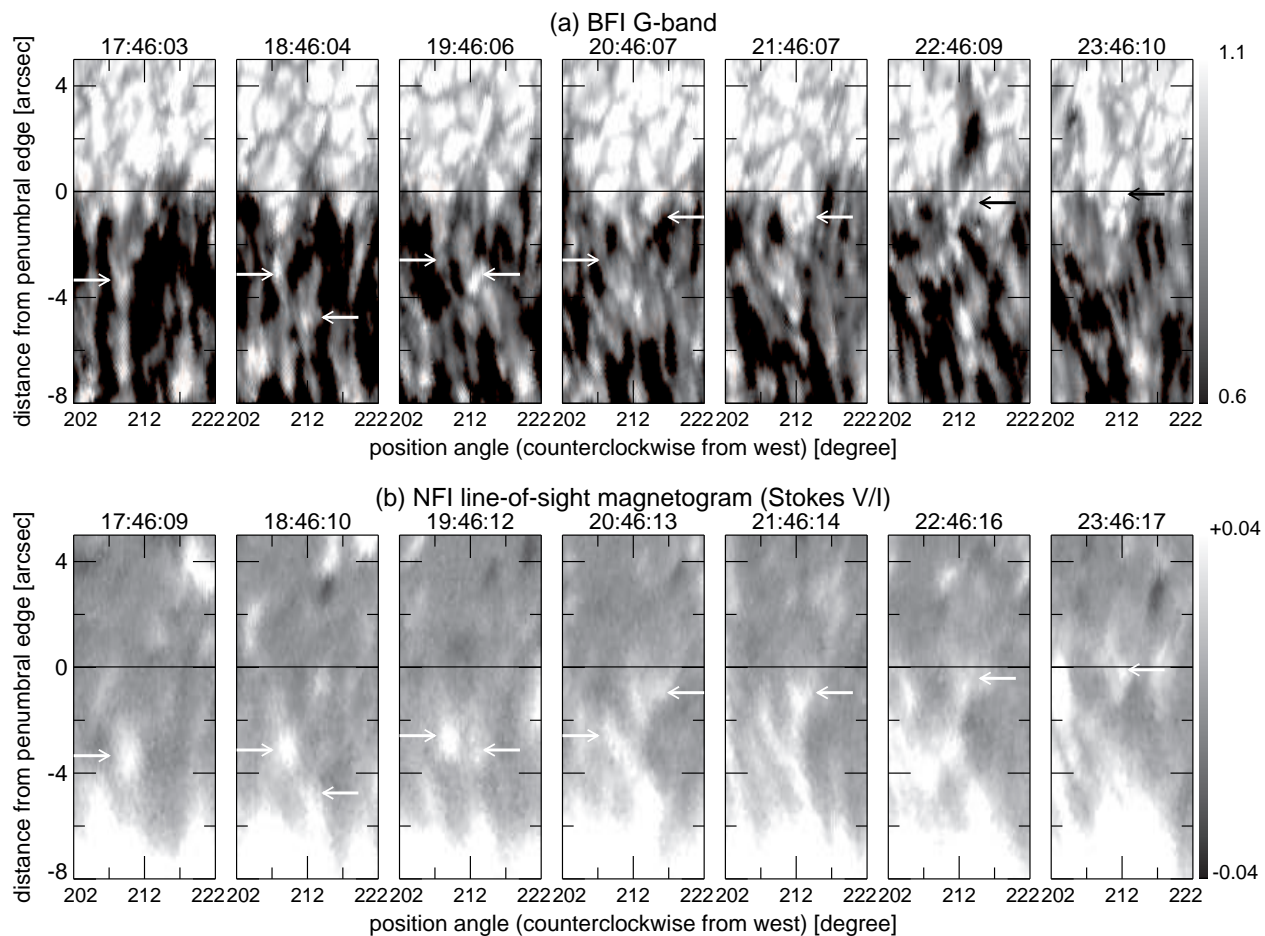


Fig. 3.— Time series of (a) G-band images and (b) line-of-sight magnetograms for position angles in the range 202° – 222° on 2007 January 4. The horizontal axis represents the position angle around the sunspot center. The vertical axis represents the radial distance from the averaged penumbral outer boundary. The horizontal solid line shows the averaged outer boundary of the penumbra. The G-band intensity is normalized to the quiet-area intensity. White indicates positive polarity and black indicates negative polarity in panel *b*. See the text for the interpretations of the arrows in the panels.

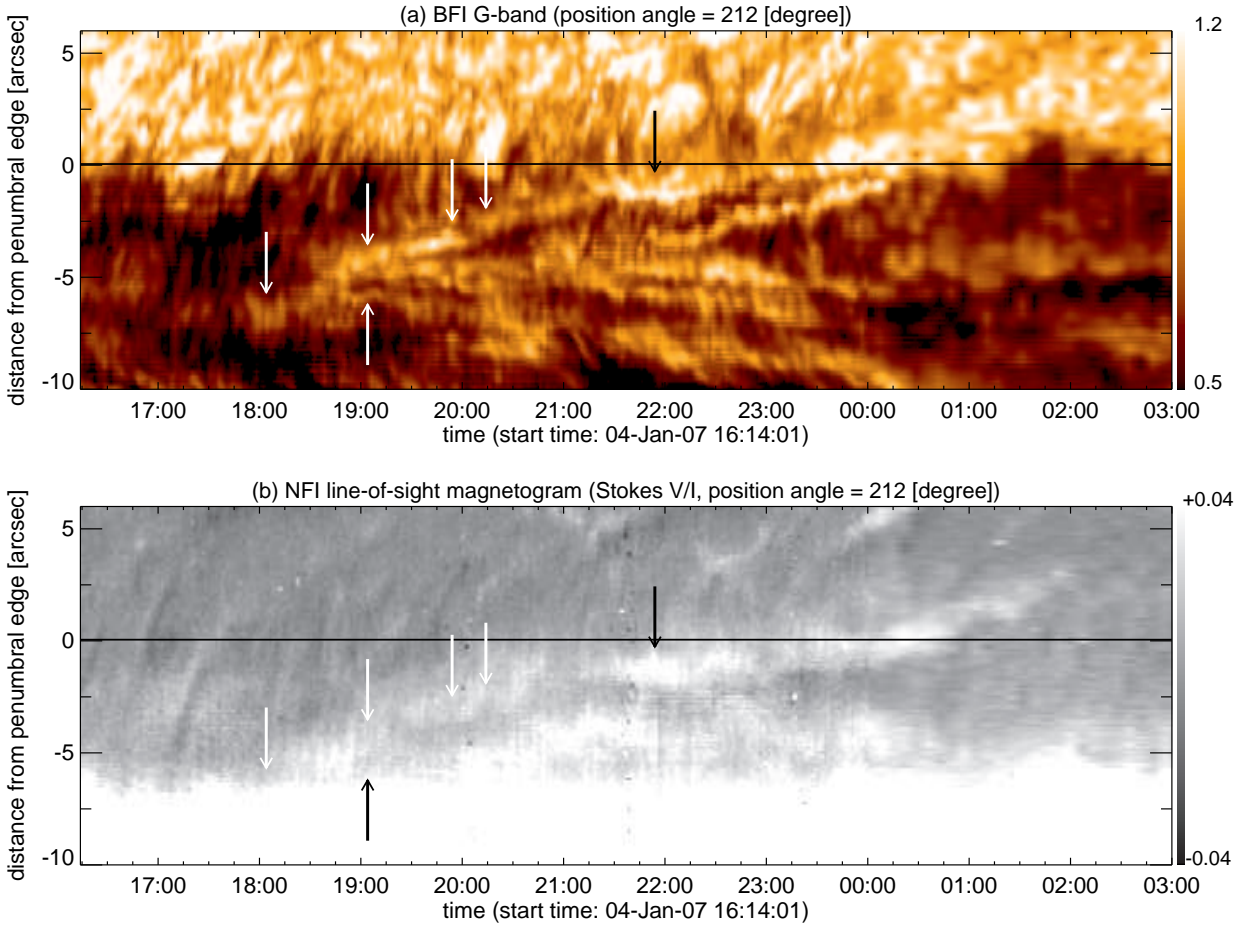


Fig. 4.— Space vs. time plots along the line at the position angle of 212° for (a) the G-band intensity and (b) the line-of-sight magnetic field. The position angle of 212° is shown by the vertical line in Fig. 2. These figures present results of two consecutive observations, differing mainly by their cadence. The cadence is 2 minutes from 16:14 to 24:00 on 2007 January 4 and is 7 minutes from 0:00 to 3:00 on 2007 January 5. The G-band intensity is normalized to the quiet-area intensity. White indicates positive polarity and black indicates negative polarity in panel *b*. See the text for the interpretation of the arrows in the panels.

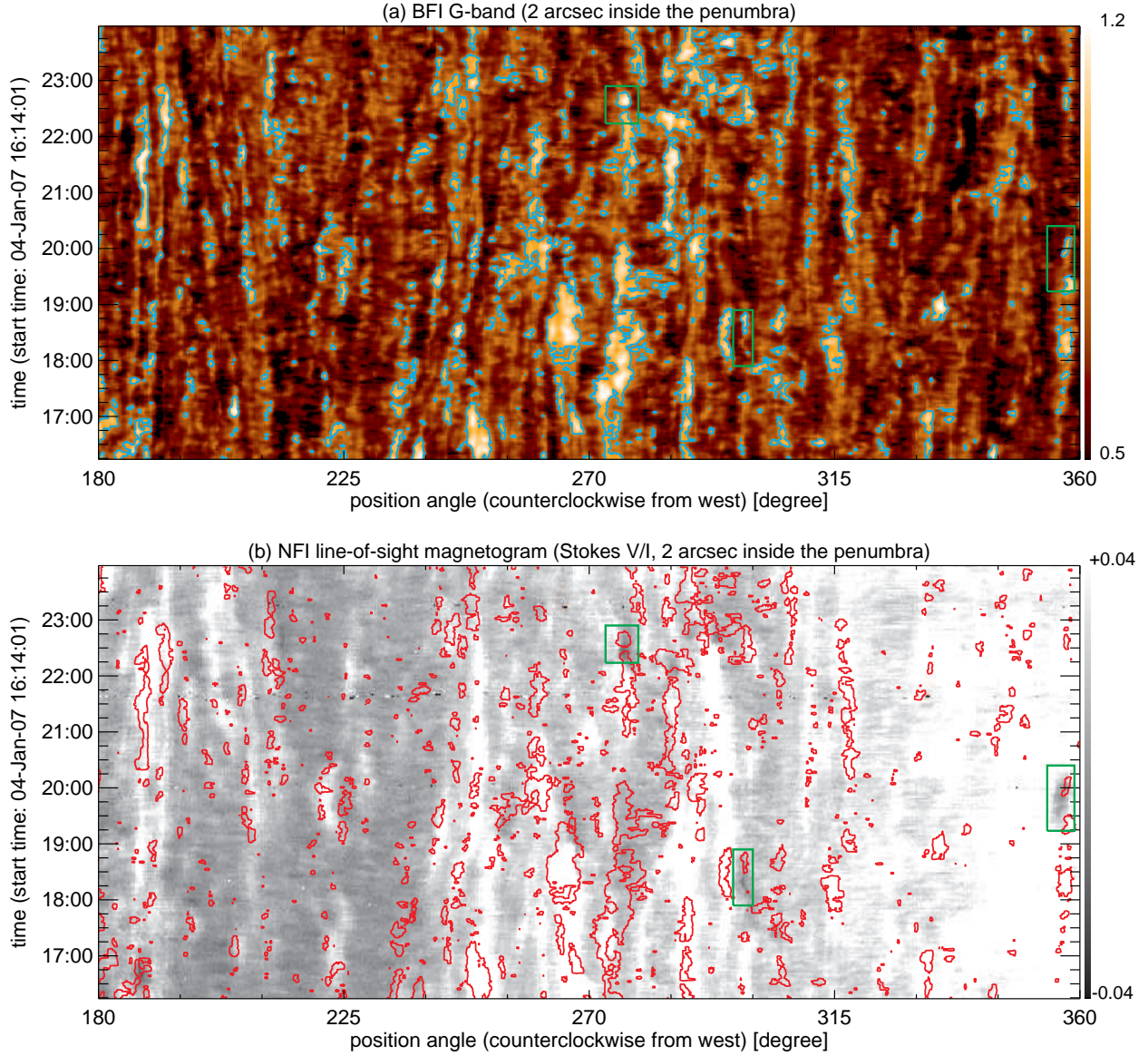


Fig. 5.— Space vs. time plots along the dashed line at $2''$ inside the penumbral outer boundary in Fig. 2 for (a) the G-band intensity and (b) the line-of-sight magnetic field. The contours represent a G-band intensity of 0.87 with respect to the quiet-area intensity. White indicates positive polarity and black indicates negative polarity in panel b. The green boxes show bright features located at the weak black areas in panel b.

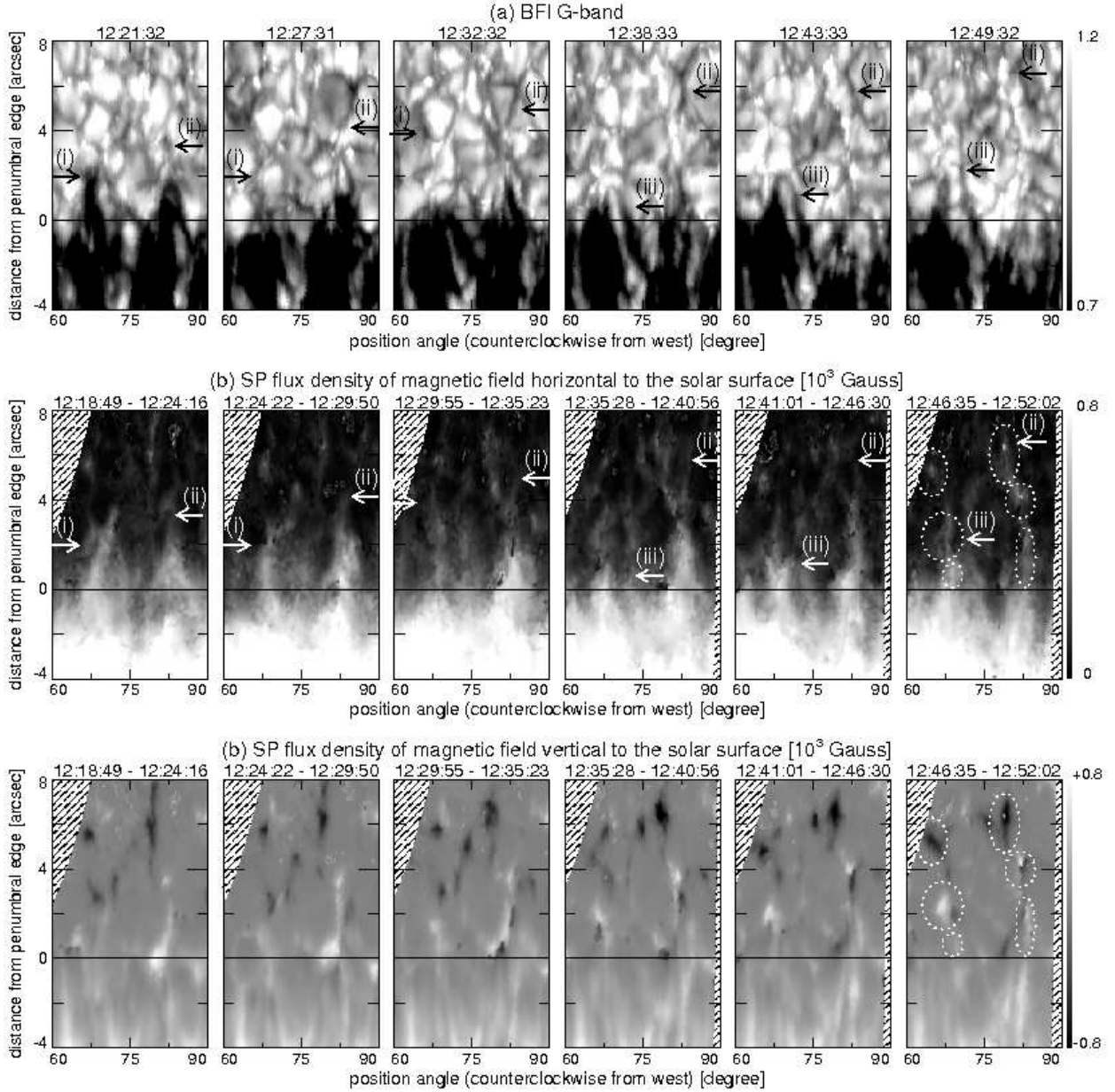


Fig. 6.— Time series of (a) the G-band images, (b) the magnetic flux density of the horizontal magnetic fields, and (c) the magnetic flux density of the vertical magnetic fields. The horizontal axis represents the position angle around the sunspot center. The vertical axis represents the radial distance from the penumbral outer boundary. These panels were obtained from the observations of NOAA AR 10944 on 2007 February 27. The magnetic flux densities of the horizontal field [$f|\mathbf{B}|\sin(\gamma)$] and the vertical field [$f|\mathbf{B}|\cos(\gamma)$] are derived from the SP observation, where the field strength is $|\mathbf{B}|$, the inclination angle with respect to the local vertical is γ , and the filling factor is f . The hatched areas with oblique lines represent the area that is out of the SP field of view. See the text for the interpretation of the arrows and circles in the panels.

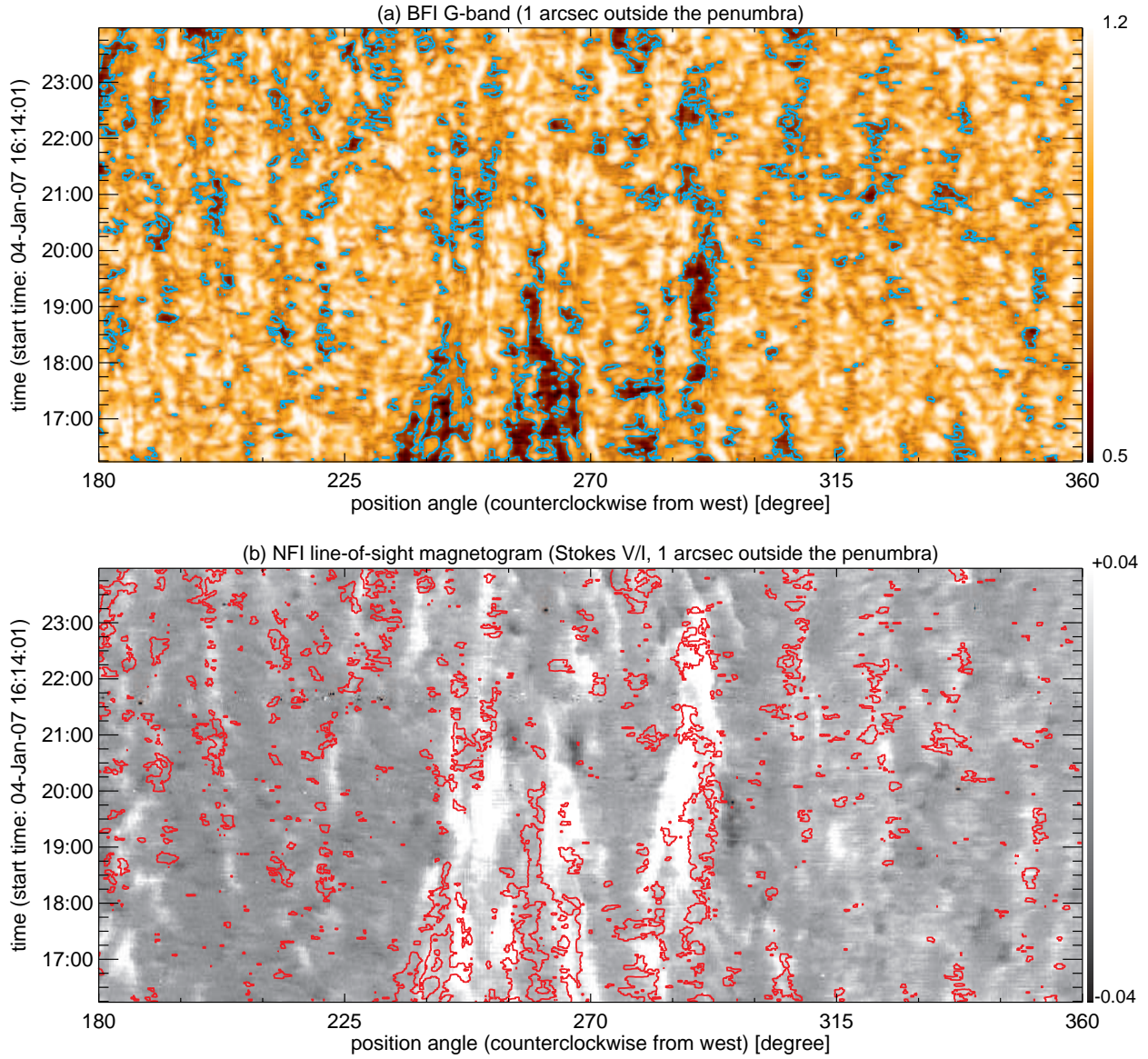


Fig. 7.— Same as Fig. 5, but for space vs. time plots at $1''$ outside the penumbral outer boundary (the dash-dotted line in Fig. 2).

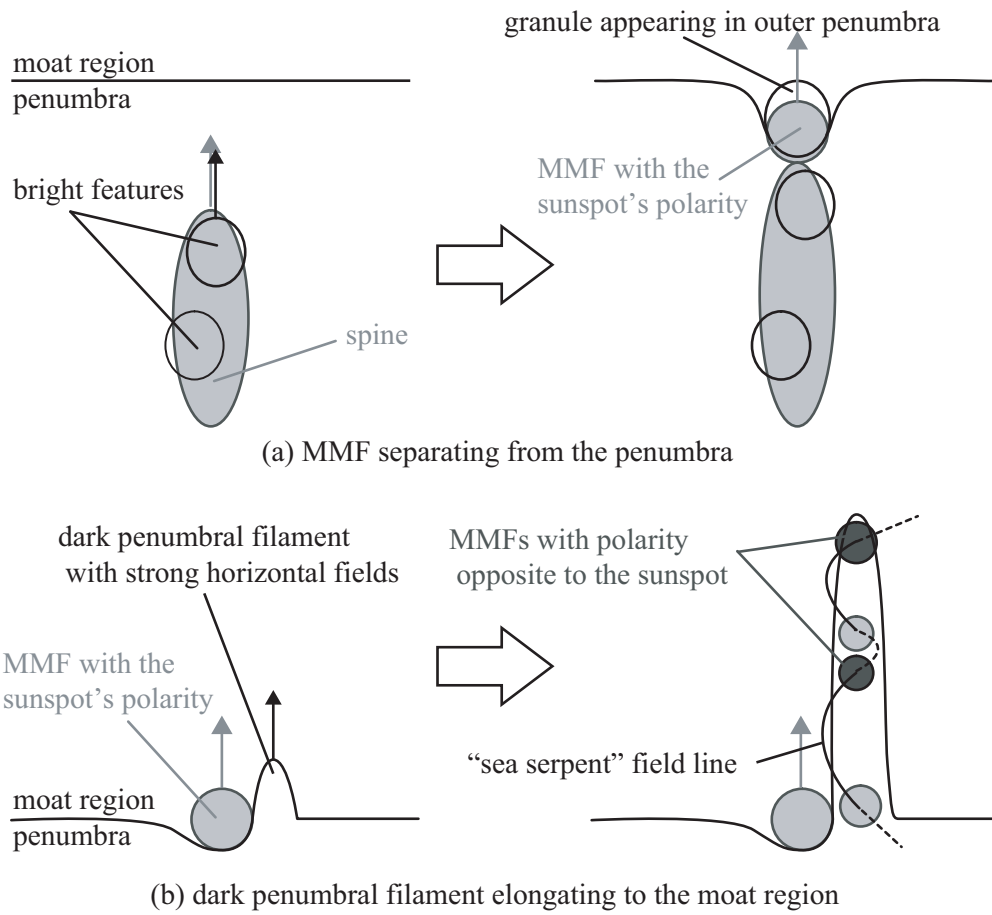


Fig. 8.— Schematic illustration for a summary of the observations around the penumbral outer boundary.